RSC Advances

ROYAL SOCIETY OF CHEMISTRY

PAPER

View Article Online
View Journal | View Issue

Cite this: *RSC Adv.*, 2022, **12**, 777

Fluorescent probe for the detection of hypochlorous acid in water samples and cell models†

Wandi Hu,[a] Mei Zhao,[a] Keyi Gu,[a] Lianwu Xie,[a] Mei Liu[b] and Danqing Lu *[a]

Hypochlorous acid (HClO) is a special kind of reactive oxygen species, which plays an important role in resisting pathogen invasion and maintaining cell redox balance and other physiological processes. In addition, HClO is commonly used in daily life as a bleaching and disinfectant agent. Its excessive use can also lead to death of water animals and serious respiratory and skin diseases in humans. Therefore, it is of great significance to develop a quick and convenient tool for detecting HClO in the environment and organisms. In this paper, we utilize the specific reaction of HClO with dimethylthiocarbamate to develop a novel naphthalene derivative fluorescent probe (**BNA-HClO**), it was designed and synthesized by using 6-(2-benzothiazolyl)-2-naphthol as the fluorophore and *N*,*N*-dimethylthiocarbamate as the recognition group. **BNA-HClO** shows large fluorescence enhancement (374-fold), high sensitivity (a detection limit of 37.56 nM), rapid response (<30 s), strong anti-interference ability and good specificity *in vitro*. Based on the outstanding *in vitro* sensing capability of **BNA-HClO**, it has been successfully used to detect spiked HClO in tap water, medical wastewater and fetal bovine serum with good recovery. **BNA-HClO** has also been successfully used as a portable test strip for the *in situ* semi-quantitative detection of HClO in tap water solutions. In addition, **BNA-HClO** can successfully enable the detection and imaging of exogenous and endogenous HClO in living cells. This work provides a simple and effective tool for the detection and imaging of HClO in environmental and biological systems, and provides some theoretical guidance for future exploration of biological and pathological studies related to HClO.

Received 5th November 2021
Accepted 15th December 2021

DOI: 10.1039/d1ra08116k

rsc.li/rsc-advances

1 Introduction

Hypochlorous acid (HClO) is a special reactive oxygen species (ROS), which is produced by myeloperoxidase (MPO)-mediated peroxidation of chloride ions and is playing an important role in killing pathogens.[1] HClO plays an important role in the human immune system. The normal concentration of hypochlorous acid in the human body is generally within the range of 200 μM.[2] When the HClO concentration in the human body dynamically fluctuates within the normal value, it can be directly used as a part of the immune defense process, which will destroy invading bacteria and pathogens. Meanwhile, the high oxidation ability of HClO makes it a double-edged sword. For example, an abnormal level HClO in organisms will cause a series of diseases, including cardiovascular disease and rheumatoid arthritis, as well as atherosclerosis and cancer.[3,4] Meanwhile, HClO that is produced by the chlorination of water ($Cl_2 + H_2O \rightarrow HClO$) is also widely used as an antimicrobial agent and disinfectant for water treatment. Unfortunately, excess HClO can result in serious harm to the environment and human health. It was reported that the use of chlorine-containing disinfectants for disinfection can increase the mortality of zebrafish embryos and increase the risk of bladder cancer in the human body.[5–7] In addition, according to the World Health Organization (WHO), the allowable upper limit of HClO in tap water is 8.6 μmol L^{-1}. Therefore, considering the potential hazard of HClO towards environment and humans, it is of great significance to develop a fast and effective method to quantify HClO in the environmental and biology.

The strategies for detecting HClO including colorimetric,[8] electrochemical,[9] chemiluminescence,[10] fluorescent probe.[11–27] Among these methods, fluorescence probe has attracted much attention owing to their various advantages over other technologies, such as simple operation, good selectivity, high sensitivity, fast response, low-cost, noninvasive detection and high spatial and temporal resolution.[28–36] In the past few years, a number of HClO fluorescent probes have been reported (see Table S1†), but only a few of them can be directly used for the real-time detection of HClO in real water samples. The main reasons are attributed to the following two points. For example, turbidity interferes more with the detection of HClO in

[a]*College of Science, Central South University of Forestry and Technology, Changsha 410004, Hunan, China. E-mail: danqinglu@csuft.edu.cn*

[b]*Ningyuan Environmental Protection Monitoring Station, Yongzhou 425600, Hunan, China*

† Electronic supplementary information (ESI) available. See DOI: 10.1039/d1ra08116k

domestic water, and while competitive interference from other active substances is greater in the biological microenvironment. On the other hand, HClO itself has high reactivity and short life. The above difficulties have greatly increased the research on the development of probes for the detection of HClO in environmental and biological systems.

Interestingly, HClO can oxidize sulfide-type amino acids, and this characteristic of HClO is different from other ROS.[37] Inspired by these characteristic, we develop a new type of fluorescent probe (**BNA-HClO**) that can be directly used for the quantitative detection of HClO in water samples and made into portable test paper to be used for highly selective monitoring HClO. The **BNA-HClO** could be easily synthesized through a one step reaction between 6-(2-benzothiazoly)-2-naphthalenol (the fluorophore) and dimethylcarbamothioic chloride (the HClO responsive site and the fluorescence quencher). The **BNA-HClO** has demonstrated high selectivity, excellent specificity, rapid response and significant fluorescence color change by investigating the analysis and detection performance of the probe in an aqueous solution. Notably, the **BNA-HClO** has been successfully applied to the detection of HClO in real water samples from remote areas (Ningyuan County Environmental Monitoring Station, Yongzhou, Hunan Province) as well as in biological fetal calf serum. The **BNA-HClO** has also been successfully prepared into a convenient test paper for highly selective quantitative monitoring of HClO in tap water. Even more importantly, the probe **BNA-HClO** allows direct *in situ* tracking of exogenous and endogenous HClO in HeLa cells.

2 Materials and methods

2.1 Synthesis and characterization

Unless otherwise stated, all reagents and solvents were of analytical grade, which were obtained directly from commercial suppliers without further purification. 6-Hydroxy-2-naphthaldehyde, 2-aminothiophenol, *p*-toluenesulfonic acid monohydrate, and dimethylcarbamothioic chloride were all purchased directly from Sigma. The secondary distilled water was used throughout all over the experiment. The ^{1}H NMR and ^{13}C NMR spectra were measured by Bruker 400 M nuclear magnetic resonance spectrometer using d_6-DMSO as the solvent, in which chemical shifts are in ppm and tetramethylsilane (TMS) is used as an internal standard. The mass spectra of different systems were measured on Bruker solanX 70 FT-MS. All fluorescence measurements were measured in the G9800A fluorescence spectrophotometer (Agilent, USA) at the slits of 5.0/5.0 nm. The pH was measured using a METTLER TOLEDO FE-28 pH; Fluorescence imaging of HeLa cells was obtained by Nikon confocal microscopy (Ti-E+A1 SI).

2.2 Synthesis and characterization

2.2.1. Synthesis of compound 1. 6-(2-Benzothiazoly)-2-naphthalenol was synthesized according to the ref. 38, which was named compound **1** in this paper. ^{1}H NMR (500 MHz, d_6-DMSO) δ (ppm): 8.55 (s, 1H), 8.15 (d, J = 7.9 Hz, 1H), 8.12–8.04 (m, 2H), 8.01 (d, J = 8.8 Hz, 1H), 7.85 (d, J = 8.6 Hz, 1H), 7.48 (d, J = 7.6 Hz, 1H), 7.21 (s, 1H), 7.13 (d, J = 8.0 Hz, 1H), 4.67 (s, 1H). ^{13}C NMR (126 MHz, d_6-DMSO) δ (ppm): 168.21, 157.65, 154.17, 138.26, 136.65, 134.83, 131.21, 128.58, 127.84, 127.59, 127.08, 125.98, 124.66, 123.08, 122.76, 120.28, 109.41. MS(EI) m/z, $C_{17}H_{11}NOS$ calcd 277.0, found $[C_{17}H_{11}NO_S]^+$ 277.0 (Fig. S1–S3†).

2.2.2. Synthesis of probe BNA-HClO. As show in Fig. 1, *N*,*N*-diisopropylethylamine (520 mg, 4 mmol) was added into compound **1** (277 mg, 1 mmol) dissolved in 20 mL dry dichloromethane and then the mixture was stirred in ice bath for 30 min to cooled to 0 °C for under N_2 atmosphere. Dimethylcarbamothioic chloride (309 mg, 2 mmol) was added to 5 mL dry dichloromethane. Then, dimethylcarbamothioic chloride in dry dichloromethane was added into the above admixture drop by drop. After stirring for 6 h in at 0 °C for under N_2 atmosphere. After the completion of the reaction (monitored by TLC), the mixture was washed in turn by 50 mL water and saturated brine and dried over anhydrous Na_2SO_4. Finally, the solvent was removed by rotary evaporation, and the residue was subsequently purified with column chromatography by petroleum ether/ethyl acetate = 15 : 1 (v/v) to afford 165 mg **BNA-HClO** as white solid with 50.0% yields. ^{1}H NMR (400 MHz, d_6-DMSO), δ (ppm): 8.73 (s, 1H), 8.25 (d, J = 8.5 Hz, 1H), 8.19 (d, J = 8.2 Hz, 2H), 8.11 (d, J = 6.3 Hz, 1H), 7.72 (s, 2H), 7.58 (t, J = 7.6 Hz, 1H), 7.50 (t, J = 7.5 Hz, 1H), 7.39 (d, J = 8.8 Hz, 1H), 3.33 (s, 6H). ^{13}C NMR (101 MHz, d_6-DMSO) δ (ppm): 186.69, 167.66, 154.10, 153.27, 135.11, 135.05, 132.01, 130.33, 129.16, 127.65, 127.21, 126.10, 124.99, 124.54, 123.35, 122.87, 119.97, 47.68. MS(EI) m/z, $C_{20}H_{16}N_2OS_2$ calcd 364.0 found $[C_{20}H_{16}N_2OS_2 + H]^+$ 365.0(Fig. S4–S6†).

2.3 Spectroscopic analysis

The **BNA-HClO** was dissolved in DMF to form a (1.0 mM) stock solution and store at 4 °C. According to the reported method. NaClO stock solution was prepared for immediate use, which was used as the source of HClO. Other species, such as KCl, NaCl, $CaCl_2$, $FeCl_3$, Na_2SO_3, $MgCl_2$, $NaNO_3$, Hcy, GSH, H_2O_2, $^1O_2$, and HNO were all dissolved in double distilled water and configured to the required concentration for selective and competitive experiments. Unless specifically stated. A stock solution of the probe **BNA-HClO** was diluted to 10 μM with 10.0 mM phosphate buffer saline (PBS/C_2H_5OH = 1 : 1, v/v, pH

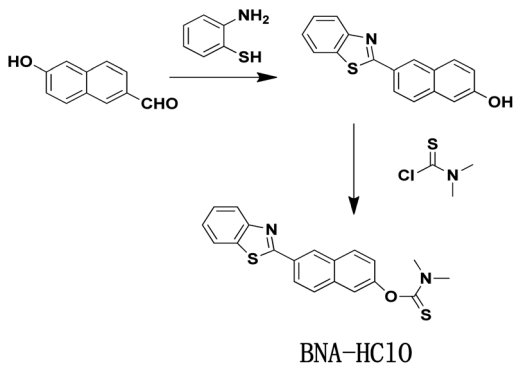

Fig. 1 The synthesis of fluorescent probe BNA-HClO.

= 7.4), and the various concentrations of HClO (0–200 μM) was added, the resulting mixture was equilibrated for 1 min at room temperature and then the fluorescence intensity was measured. The excitation wave-length was set at 384 nm, the emission spectra were scanned from 450 nm to 600 nm, and both excitation and emission slit widths were set at 5 nm. The fluorescence spectra were collected at a wavelength of 510 nm, the data of these experiments were reported as the mean ± standard deviation of triplicate experiments. Other optical experiments were similar.

3 Results

3.1 Desigh strategy of probe

In this work, an ICT-based fluorescent probe named **BNA-HClO** was rationally designed and synthesized for the special response to HClO. The generation of "push–pull" fluorescent structure induced by the specific reaction of HClO was adopted to enhance the sensitivity. The naphthalene hydroxyl derivative was selected as a fluorophore by virtue of its high fluorescence quantum yield, effective two-photon active absorption cross-section, high photostability, concise synthesis, and easy modification which may offer a perfect platform for constructing two-photon fluorescence probe. Furthermore, it has been reported that sulfide-type amino acids can be oxidized through the initiation of an electrophilic addition of Cl^+ which from the decomposition of HClO.[39–41] Therefore, we selected dimethylcarbamothioic chloride with a strong intromolecular charge transfer effect (ICT) as the HClO reactive group and the fluorescence quencher. As a consequence, based on the oxidation of HClO, *N*,*N*-dimethylthiocarbamate was removed, releasing the D–π–A structure of naphthalene derivatives as well as the fluorescence recovering (Fig. 2). Therefore, probe **BNA-HClO** can recognize HClO selectively.

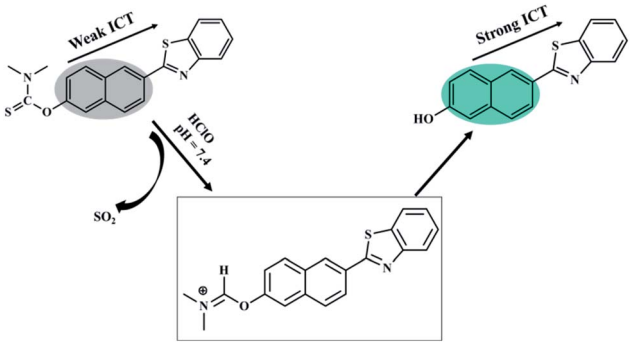

Fig. 2 Possible recognition mechanism of fluorescent probe for HClO.

3.2 Fluorescence response of probe BNA-HClO toward HClO

In order to inquire the ability of **BNA-HClO** to qualitatively and quantitatively detect HClO, we first tested the UV-vis spectra response **BNA-HClO** toward HClO. As shown in Fig. S7,† **BNA-HClO** exhibited an maximum absorption peak at a wavelength (λ_{abs}) of 340 nm ($\varepsilon = 1972\ M^{-1}\ cm^{-1}$), upon addition of HClO to probe **BNA-HClO** solution, the maximum absorption spectrum of probe **BNA-HClO** was slightly red-shifted to 384 nm (ε = 2825 $M^{-1}\ cm^{-1}$). However, the change between the maximum absorption wavelength of probe **BNA-HClO** and HClO before and after response was not obvious. Therefore, the following studies were focus on the fluorescence method. The probe **BNA-HClO** was investigated for fluorescence detection of HClO in PBS/C_2H_5OH (1 : 1, v/v, pH = 7.4), due to the inhibiting of intramolecular charge transfer (ICT) process between fluorophore and quencher. The probe **BNA-HClO** was essentially non-fluorescent in the absence of HClO ($\phi = 0.10$). Nevertheless, the fluorescence intensity of probe **BNA-HClO** significantly increased at 510 nm ($\phi = 0.57$) as the HClO concentration increased from 0 to 200 μM (Fig. 3a). When the HClO concentration reached 200 μM, the fluorescence intensity of probe **BNA-HClO** reached a plateau, which was 374 folds the blank value. As shown in Fig. 3b, the fluorescence emission of probe **BNA-HClO** has a good linear relationship with the HClO for

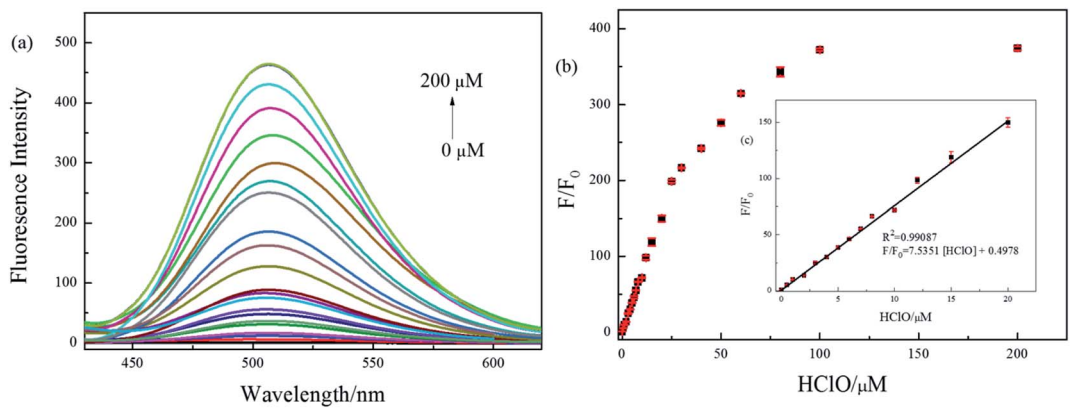

Fig. 3 (a) Fluorescence emission spectra of the probe (10 μM) in the presence of different concentrations of HClO (0–200 μM). (b) The calibration curve of the sensing system, inset exhibits the linear response at low concentration of HClO (0–20 μM). *F* and F_0 represent the fluorescence intensity of the presence or absence of HClO. PBS buffer solution system (10 mM, pH 7.4, C_2H_5OH/PBS = 1 : 1, v/v), λ_{ex} = 384 nm, λ_{em} = 450–600 nm.

concentrations of HClO ranging from 0 to 20 μM. The regression equation was $F/F_0 = 7.5351$ [HClO] + 0.4978, with $R^2 = 0.9909$. Moreover, the detection limit of probe **BNA-HClO** for HClO was estimated to be as low as 37.54 nM according to LOD $= 3\delta/k$, where σ is means of the standard deviation of the blank measures, and k is a numerical slope factor between the fluorescent intensity and the concentrations of HClO. These results showed that probe **BNA-HClO** could be used to measure HClO quantitatively in a wide linear range.

3.3 Time – dependence in the detection process of HClO

HClO has the characteristics of high reactivity and short life. Whether **BNA-HClO** responds quickly to HClO is the key point to determine whether the probe can accurately detect HClO. Therefore, we also tested the reaction time of probe **BNA-HClO** and HClO under physiological conditions. As shown in Fig. 4, with HClO (100 μM) added to **BNA-HClO** (10 μM), the probe immediately shows strong fluorescence emission at 510 nm within 30 s, which shows that probe **BNA-HClO** responded to HClO fast and sensitively. The fluorescence intensity of probe **BNA-HClO** with HClO remained stable for the next 240 s, indicating that the fluorescence stability of probe **BNA-HClO** was perfect. In contrast, the probe **BNA-HClO** without HClO did not show any obvious fluorescence change within 240 s.

3.4 Effect of pH

We also investigated the effect of pH to probe **BNA-HClO**. As shown in Fig. 5, the probe itself had no influence on the fluorescence by the pH of mediums within the range from 5.0 to 9.0. In the presence of HClO (100 μM), the fluorescence intensity of probe **BNA-HClO** gradually increased during the pH raising (5.0–7.4). However, the fluorescence intensity obviously decreased in the pH = 8.0–9.0 for which the reaction was inhibited, but the signal-to-noise ratio is relatively obvious. The main reason may be that the reaction between the added HClO specificity and probe **BNA-HClO** leads to the restoration of the push–pull electronic structure of probe **BNA-HClO**, so the fluorescence intensity of probe **BNA-HClO** increases significantly. However, the alkaline reaction system will inhibit the reaction and weaken the fluorescence intensity of the system.[36] However, under physiological conditions (pH = 7.4), the fluorescence signal to back ratio enhancement of the probe **BNA-HClO** is significantly higher up to 374-fold. Thus, the probe **BNA-HClO** has the potential to detect HClO in a biological environment.

3.5 Selectivity and competition experiments

For an excellent probe, a high selectivity is required. To do this, various analytes including HClO (100 μM) and other potential interfering substances such as (1 mM) KCl, NaCl, $CaCl_2$, $FeCl_3$, Na_2SO_3, $MgCl_2$, $NaNO_3$, Hcy, GSH, H_2O_2, $^1O_2$, HNO were added to the probe **BNA-HClO** solution. As shown in Fig. 6, only addition of HClO induced the fluorescence intensity of probe **BNA-HClO** solution increased significantly at 510 nm while other analytes induced negligible changes, which indicates that probe **BNA-HClO** has high selectivity for HClO over other potential interfering substances. To further assess its utility as a HClO selective fluorescent probe, its fluorescence spectrum response to HClO in the presence of other species mentioned above was also tested. As shown in Fig. 7, the fluorescence response of probe **BNA-HClO** to HClO in the presence of other potential interfering substances (1 mM KCl, NaCl, $CaCl_2$, $FeCl_3$, Na_2SO_3, $MgCl_2$, $NaNO_3$, Hcy, GSH, H_2O_2, $^1O_2$, HNO) was studied, and no obvious interference was detected. All these results indicate that probe **BNA-HClO** is selective for HClO and promising for detection of HClO in complex environmental conditions.

3.6 Proposed detection mechanism of probe

In order to assess the sensing mechanism of **BNA-HClO** toward HClO, the reaction system was verified by HPLC and MS spectra methods. The HPLC analysis showed that the reaction mixture produced a fluorescence compound, which has the same retention time to compound **1**. Comparing the three pictures in Fig. S8a,† it could be seen that after probe **BNA-HClO** and HClO reacted for 1 min, the signal of compound **1** was significantly

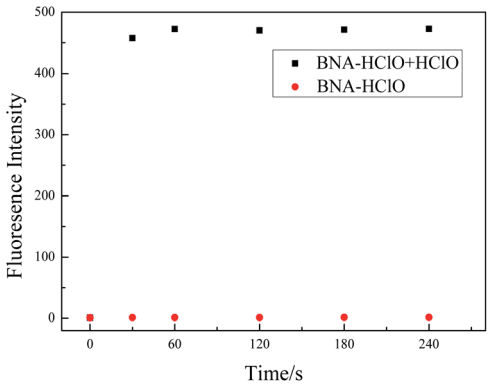

Fig. 4 The time-dependent fluorescence spectra of probe **BNA-HClO** responses to HClO. Data were acquired in 10.0 mM PBS/C_2H_5OH (1 : 1, v/v, pH 7.4). Fluorescence signals with $\lambda_{ex} = 384$ nm, $\lambda_{em} = 510$ nm.

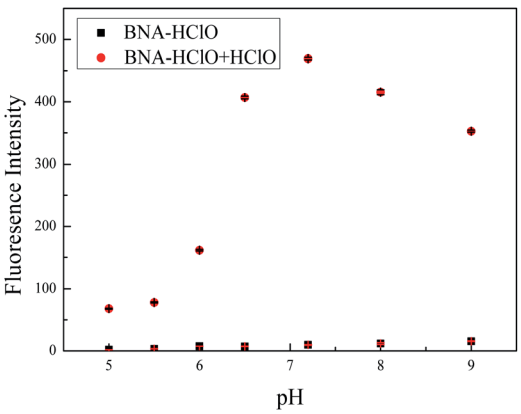

Fig. 5 The effect of different pH on the fluorescence intensity of the probe **BNA-HClO** (10.0 μM) toward HClO (100.0 μM); data were acquired in 10.0 mM PBS/C_2H_5OH (1 : 1, v/v, pH 7.4). Fluorescence signals with $\lambda_{ex} = 384$ nm, $\lambda_{em} = 510$ nm.

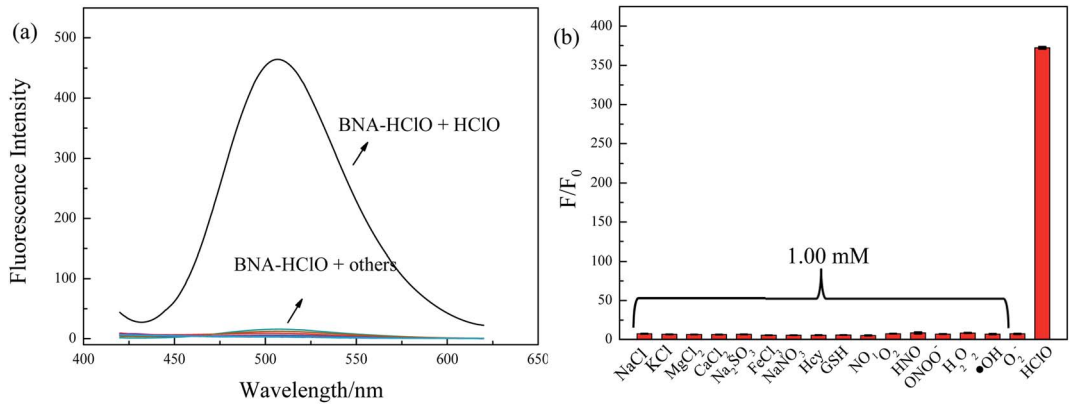

Fig. 6 Selective investigation of probe **BNA-HClO**. (a) Fluorescence emission spectra of **BNA-HClO** in response to different substances, (b) F/F_0 of **BNA-HClO** in response to different substances.

increased, indicating that the reaction of probe **BNA-HClO** and HClO did produce compound **1**. At the same time, the product was characterized by ESI-MS spectrometry. As shown in Fig. S8b,† a new peak appeared at 278.95 (m/z) in the spectrum, suggesting that the transformation from probe **BNA-HClO** to compound **1** ([M + H]+m/z calcd 278.06) was induced by HClO. The response mechanism of probe **BNA-HClO** verified by the two experimental results at the same time indicated that the enhanced fluorescence of probe **BNA-HClO** was indeed due to sulfide-type amino acids can be oxidized through the initiation of an electrophilic addition of Cl^+ which from the decomposition of HClO, restoring the D–π–A structure of the naphthalene derivative and the fluorescence.

3.7 Real sample analysis

Hypochlorous acid is an important bioactive oxygen species that plays a vital role in the human immune system; it is also widely used in the natural environment as a disinfectant and bleaching agent for tap water and medical wastewater. For example, in disinfection of tap water, medical wastewater, and daily life. HClO is used at a concentration in the range of 10^{-5} to 10^{-2} M.[42] Therefore, whether the probe **BNA-HClO** can be directly used for the detection of HClO in actual domestic water samples and biological systems is a key point to evaluate the performance of this probe. In this experiment, tap water, medical wastewater and serum were selected as the reaction media for the study, and the practical application of the probe **BNA-HClO** was investigated separately. Both tap water and medical wastewater are provided by the Yongzhou Environmental Testing Station, which were filtered through filter paper ($\Phi = 7$ cm) to remove impurities during the measurement, and the medical sewage is diluted 10 times with double distilled water before the measurement. Therefore, according to the linear regression equation (Fig. 3b), the results of the determination of HClO in water samples and the results of spiked recovery experiments was shown in Table 1: the HClO levels in fetal bovine serum, tap water, and medical wastewater were non-detect, 2.98 μM, and 93.0 μM, respectively. The test results were within the standard ranges for tap water discharge (8.6 μM)[43] and medical wastewater discharge (123–190 μM).[44] The recoveries of all spiked standards were in the range of 96.1–102.7%, which proved the validity and accuracy of the method for the detection of HClO. The above results indicate that the probe **BNA-HClO** has the potential to be used for the detection of HClO in environmental water samples and biological systems.

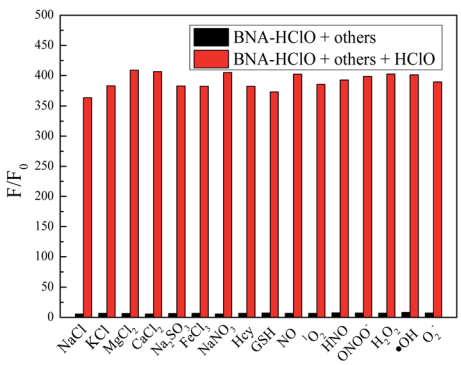

Fig. 7 Investigation of anti-jamming ability of probe **BNA-HClO**.

Table 1 Detection of HClO in actual water samples by **BNA-HClO** probe

Sample	Determined[a] (μM)	Added HClO (μM)	Found[a] (μM)	Recovery (%)
1	ND	2.00	2.05 ± 0.01	102.4
		5.00	4.97 ± 0.06	99.4
		10.00	9.61 ± 0.06	96.1
2	2.98 ± 0.05	2.00	5.02 ± 0.03	102.0
		5.00	8.09 ± 0.04	102.3
		10.00	12.90 ± 0.09	98.0
3	9.30 ± 0.07	2.00	11.36 ± 0.02	102.6
		5.00	14.44 ± 0.04	102.7
		10.00	19.90 ± 0.08	96.6

[a] Mean ± standard deviation ($n = 3$).

3.8 Paper test strips

The above experimental results all prove the outstanding sensitivity and excellent selectivity of **BNA-HClO** for the detection of HClO. Therefore, we have prepared a portable test paper that can be directly used for the determination of HClO in the environment, and explored the specificity and qualitative and quantitative analysis performance of the test paper for HClO. The filter paper was first cut into circular pieces of paper with a diameter of 15 cm, and then inserted into the probe solution with a concentration of 10 μM for 30 minutes, and finally dried naturally. Firstly, when the aqueous solutions containing 100 μM HClO and 1 mM KCl, NaCl, $CaCl_2$, $FeCl_3$, Na_2SO_3, $MgCl_2$, $NaNO_3$, Hcy, GSH were dropwise added onto the test strips at room temperature respectively, and the fluorescence change of the test paper under UV lamp (365 nm) by naked eyes was recorded. As shown in Fig. 8a, only when HClO is added to the test paper, the test paper exhibits strong green fluorescence under UV lamp (365 nm). Secondly, the test paper is used to detect different concentrations of HClO. As shown in Fig. 8b, the fluorescent color of the test paper changes from blue to green under UV lamp (365 nm), and the fluorescence is continuously enhanced. In addition, the dried test paper is directly immersed in pretreated tap water. The color of the test paper is compared with the standard color card (Fig. 8b), which met the standards of the required concentrations in tap water. These results indicated that the test paper is not only convenient to carry, sensitive to identification, capable of semi-quantitative *in situ* identification of HClO, and has important significance for monitoring the HClO in tap water or other environmental water samples.

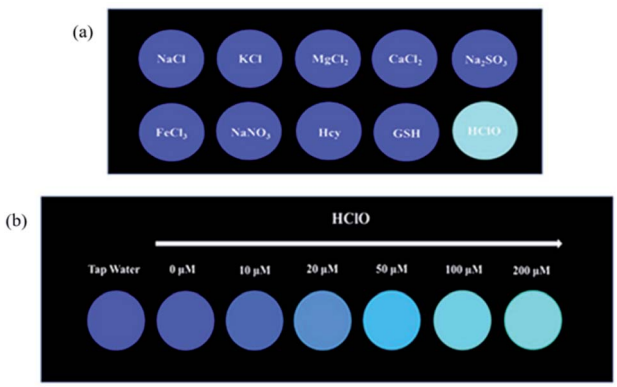

Fig. 8 (a) Fluorescence images of test paper soaked with probe **BNA-HClO** to detection interfering substances (1 mmol L^{-1}) and HClO (100 μmol L^{-1}) under 365 nm, (b) fluorescence images of test paper soaked with probe **BNA-HClO** to detection HClO (0–200 μmol L^{-1}) in water under 365 nm.

3.9 Cytotoxicity studies

To ensure the safety of probe **BNA-HClO** for bioimaging studies, the toxicity of probe **BNA-HClO** and compound **1** on HeLa cells were first assessed by the CCK-8 method. As seen in Fig. 9, when (0–12 μM) probe **BNA-HClO** was co-incubated with cells for 48 h, HeLa cell viability decreased from 102.50% to 94.24%. The survival rate was higher than 90%, meanwhile, when (0–12 μM) compound **1** was co-incubated with HeLa cells for 48 h, the HeLa cell viability decreased from 103.60–92.35%, and the cell survival rate was also higher than 90%. And as seen in Fig. S9,† the higher concentrations of the probe **BNA-HClO** (15–30 μM) also have good cellular compatibility. The above experimental results shown that the probe **BNA-HClO** and compound **1** did not exhibit significant cytotoxicity to HeLa cells within the experimentally investigated concentration range, indicating that the probe **BNA-HClO** has good cytocompatibility and can be directly used for the detection and imaging studies of HClO in biological systems.

3.10 Cell imaging

The results of *in vitro* experiments and cytotoxicity assays demonstrated the good sensitivity, specificity, and cytocompatibility of the probe **BNA-HClO** in detecting HClO. Therefore, the imaging of exogenous and endogenous HClO in HeLa cells with the probe **BNA-HClO** was investigated by fluorescence confocal microscopy. In the detection of exogenous HClO in live cells, it can be seen from Fig. 10a–c that only the probe **BNA-HClO** (10 μM) and HeLa cells were incubated for

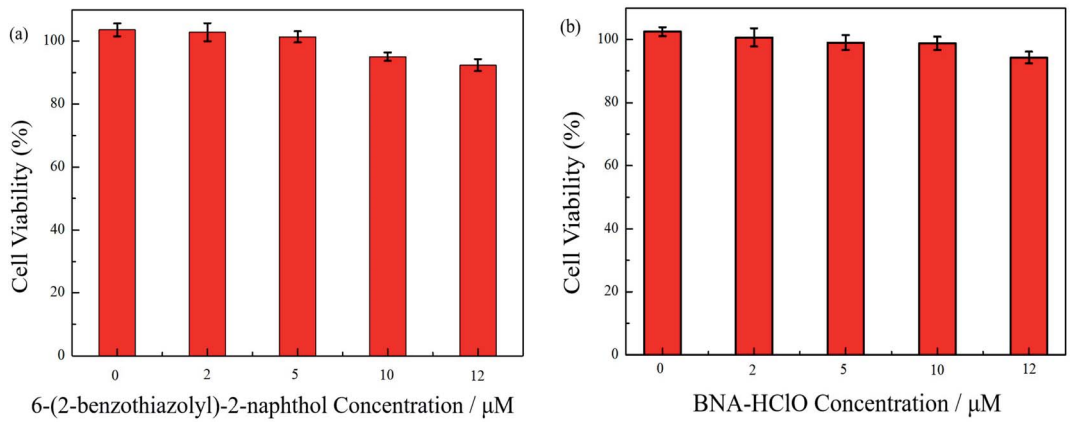

Fig. 9 Cytotoxicity of compound **1** (a) and probe **BNA-HClO** (b).

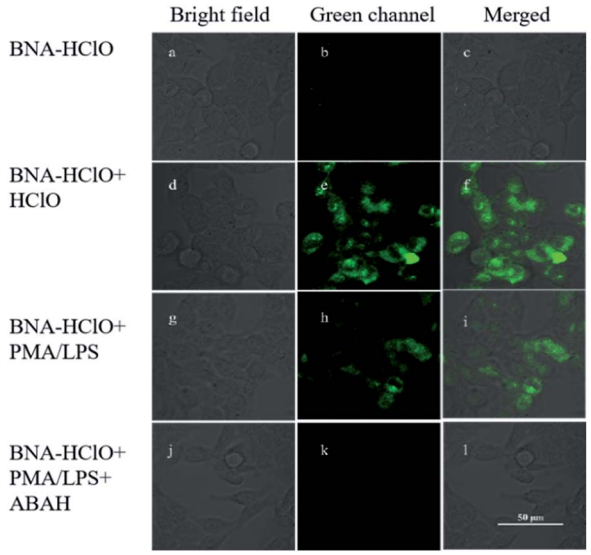

Fig. 10 Confocal fluorescence imaging of the probe **BNA-HClO** with exogenous and endogenous HClO in HeLa cells. (a–c) The imaging of HeLa cells treated with **BNA-HClO** (10 μM) for 30 min; (d–f) The imaging of HeLa cells treated with 10.0 μM **BNA-HClO** for 30 min and then treated with 40 μM HClO for 30 min; (g–i) The imaging of HeLa cells were incubated with LPS (1.0 μg mL^{-1}) for 12 h, and then were incubated with PMA (1.0 μg mL^{-1}) for 1 h, and finally probe **BNA-HClO** (10 μM) was added incubate for 30 min; (j–l) HeLa cells were first incubated with ABAH (200 μM) for 3 h, then with LPS (1.0 μg mL^{-1}) for 12 h, and incubate with PMA (1.0 μg mL^{-1}) for 1 h, and finally incubate with **BNA-HClO** (10 μM) for 30 min. The fluorescence intensities were collected at the green channel (490–550) upon excitation at 800 nm. Scale bar: 50 μm.

30 min, and the probe **BNA-HClO** had no obvious fluorescence in the cells under the excitation light of 405 nm. However, when HeLa cells were incubated with the probe **BNA-HClO** (10 μM) and continued with the addition of exogenous HClO (40 μM) for 30 min, the green fluorescence of HeLa cells increased significantly (Fig. 10d–f). The above experimental results indicate that the probe **BNA-HClO** has good cytocompatibility and membrane permeability and has the potential to detect exogenous HClO in living cells. In order to further explore the potential of probe **BNA-HClO** to detect HClO in biological environment, this experiment further applied probe **BNA-HClO** to detect endogenous HClO in living cells. HeLa cells were first pretreated with LPS(μg mL^{-1}) and PMA (μg mL^{-1}) stimulation to produce endogenous HClO, a clear green fluorescence enhancement was observed in the HeLa cells after continued incubation with the probe **BNA-HClO** (10 μM) (Fig. 10g–i). Meanwhile, to confirm that the fluorescence signal was mainly caused by endogenous HClO produced by LPS and PMA stimulation, this experiment used ABAH as an inhibitor of MPO enzyme activity to reduce the production of endogenous HClO by cells. As shown in Fig. 10j–l, HeLa cells were first incubated with ABAH and then incubated with LPS, PMA and the probe **BNA-HClO** in sequence, the results were compared with Fig. 10g–i, the cell fluorescence intensity was significantly weakened, which proved that the change of the probe fluorescence signal was caused by the intracellular production of endogenous HClO. The above experimental results indicate that the probe **BNA-HClO** can also be used for imaging and analysis of endogenous HClO in living cells.

4 Conclusion

In this paper, the probe **BNA-HClO** was successfully synthesized based on the ICT mechanism using *N*,*N*–dimethylthiocarbamate bond as the recognition group and fluorescence quenching group. The probe **BNA-HClO** has the advantages of rapid response, high sensitivity, good selectivity, strong anti-interference ability, the detection limit of the probe **BNA-HClO** is 37.5 nM, which is much lower than the threshold limit set by the National Standardization Administration. What's more, the probe **BNA-HClO** can be directly used for the detection of HClO in tap water, medical wastewater and biological serum systems. The probe **BNA-HClO** was further successfully made into a portable test strip, which has the ability of semi-quantitative analytical detection. In addition, the probe **BNA-HClO** was successfully used for the imaging analysis of exogenous and endogenous HClO in living cells. In conclusion, the probe **BNA-HClO** provides a favorable tool for the study of HClO at the practical application level.

Informed consent statement

Informed consent was obtained from all subjects involved in the study.

Author contributions

Conceptualization, D. Q. L. and M. Z.; methodology, M. Z. and D. Q. L; validation, M. Z. and K. Y. G; investigation, W. D. H., M. Z and K. Y. G; resources, D. Q. L. and M. L.; data curation, W. D. H., M. Z. and K. Y. G; writing—original draft preparation, M. Z. and W. D. H.; writing—review and editing, W. D. H, L. W. X and D. Q. L; supervision, D. Q. L. All authors have read and agreed to the published version of the manuscript.

Conflicts of interest

There are no conflicts to declare.

Acknowledgements

This work was funded by the National Natural Science Foundation for Young Scientists of China (Grant 22004132), Natural Science Foundation for Young Scientists of Hunan Province (Grant 2020JJ5963), Provincial Key Research and Development Plan in Hunan, China (2020NK2019). Scientific Innovation Fund for Post-graduates of Central South University of Forestry and Technology, China (CX202102076).

References

1 Z. M. Prokopowicz, F. Arce, R. Biedroń, C. L. Chiang, M. Ciszek, D. R. Katz, M. Nowakowska, S. Zapotoczny,

J. Marcinkiewicz and B. M. Chain, *J. Immunol.*, 2010, **184**, 824–835.
2 S. Hammerschmidt, N. Büchler and H. Wahn, *Chest*, 2002, **121**, 573.
3 S. M. Wu and S. V. Pizzo, *Arch. Biochem. Biophys.*, 2001, **391**(1), 119.
4 D. I. Pattison and M. J. Davies, *Biochemistry*, 2006, **45**, 8152.
5 M. L. Kent, C. Buchner, C. Barton and R. L. Tanguay, *Dis. Aquat. Org.*, 2014, **107**(3), 235–240.
6 L. E. Beane Freeman, K. P. Cantor, D. Baris, J. R. Nuckols, A. Johnson, J. S. Colt, M. Schwenn, M. H. Ward, J. H. Lubin, R. Waddell, G. M. Hosain, C. Paul, R. McCoy, L. E. Moore, A. T. Huang, N. Rothman, M. R. Karagas and D. T. Silverman, *Environ. Health Perspect.*, 2017, **125**(6), 067010.
7 S. E. Hrudey, L. C. Backer, A. R. Humpage, S. W. Krasner, D. S. Michaud, L. E. Moore, P. C. Singer and B. D. Stanford, *J. Toxicol. Environ. Health, Part B*, 2015, **18**(5), 213.
8 J. Zhang, X. Wang and X. Yang, *Analyst*, 2012, **137**, 2806.
9 S. Thiagarajan, Z. Y. Wu and S. M. Chen, *J. Electroanal. Chem.*, 2011, **661**(2), 322–328.
10 G. J. Mao, Y. Y. Wang, W. P. Dong, H. M. Meng, Q. Q. Wang, X. F. Luo, Y. Li and G. Zhang, *Spectrochim. Acta, Part A*, 2021, **249**, 119326.
11 L. He, H. Q. Xiong, B. H. Wang, Y. Zhang, J. P. Wang, H. Y. Zhang, H. P. Li, Z. G. Yang and X. Z. Song, *Anal. Chem.*, 2020, **92**, 11029.
12 Y. Jiang, G. Zheng, Q. Duan, L. Yang, J. Zhang, H. Zhang, J. He, H. Sun and D. Ho, *Chem. Commun.*, 2018, **54**(57), 7967–7970.
13 X. L. Jin, Y. F. Jin, W. X. Chen, P. Chui and Z. H. Yang, *Sens. Actuators, B*, 2016, **232**, 300–305.
14 Y. W. Jun, S. Sarkar, S. Singha, Y. J. Reo, H. R. Kim, J. J. Kim, Y. T. Chang and K. H. Ahn, *Chem. Commun.*, 2017, **28**, 10800.
15 X. Y. Li, L. Wu, Z. Y. Zhao, C. Y. Liu and B. C. Zhu, *RSC Adv.*, 2019, **9**, 4659–4664.
16 C. Y. Liu, P. Jia, L. Wu, Z. L. Li, H. C. Zhu, Z. K. Wang, S. Deng, W. Shu, X. Zhang, Y. M. Yu and B. C. Zhu, *Sens. Actuators, B*, 2019, **297**, 126731.
17 L. F. Pang, Y. M. Zhou, W. L. Gao, H. H. Song, X. Wang and Y. Wang, *RSC Adv.*, 2016, **6**, 105795.
18 L. Shi, H. J. Yu, X. Q. Zeng, S. Yang, S. Z. Gong, H. Xiang, K. Zhang and G. Shao, *New J. Chem.*, 2020, **44**, 6232.
19 X. Wang, Y. Zhou, C. Xu, H. Song, L. Li, J. Zhang and M. Guo, *Spectrochim. Acta, Part A*, 2018, **203**, 415.
20 L. L. Wu, Q. Y. Yang and L. Y. Liu, *Chem. Commun.*, 2018, **54**(61), 8522–8525.
21 Y. Zhang, X. Q. Zhang, H. C. Yang, L. Yu, Y. J. Xu, A. Sharma, P. Yin, X. Y. Li, J. S. Kim and Y. Sun, *Chem. Soc. Rev.*, 2021, **50**, 11227.
22 X. Yang, Q. H. Ou, K. Qian, J. R. Yang, Z. X. Bai, W. Y. Yang, Y. M. Shi and G. Liu, *Coordin. Chem. Rev.*, 2021, **443**, 214017.
23 P. Z. Wang, H. C. Yang, C. Liu, M. Q. Qiu, X. Ma, Z. Q. Mao, Y. Sun and Z. H. Liu, *Chin. Chem. Lett.*, 2021, **32**, 168.
24 F. Ding, Z. Chen, W. Y. Kim, A. Sharma, C. L. Li, Q. Y. Ouyang, H. Zhu, G. F. Yang, Y. Sun and J. S. Kim, *Chem. Sci.*, 2019, **10**, 7023.
25 K. Wang, D. Xi, C. Liu, *et al.*, *Chin. Chem. Lett.*, 2020, **31**(11), 2955–2959.
26 J. Ouyang, Y. F. Li, W. L. Jiang, S. Y. He, H. W. Liu and C. Y. Li, *Anal. Chem.*, 2019, **91**, 1056–1063.
27 W. J. Huang, H. C Yang, Z. X. Hu, Y. F. Fan, X. F. Guan, W. Q. Feng, Z. H. Liu and Y. Sun, *Adv. Healthcare. Mater.*, 2021, **10**, 2101003.
28 L. He, H. Q. Xiong and B. H. Wang, *Anal. Chem.*, 2020, **16**, 11029–11034.
29 Y. Jiang, G. S. Zheng and Q. Y. Duan, *Chem. Commun.*, 2018, **54**(57), 7967–7970.
30 X. L. Jin, Y. F. Jia and W. X. Chen, *Sens. Actuators, B*, 2016, **232**, 300–305.
31 Y. W. Jun, S. Sarkar and S. Singha, *Chem. Commum.*, 2017, **53**(78), 10800–10803.
32 X. Y. Li, L. Wu and Z. Y. Hao, *RSC Adv.*, 2019, **9**(8), 4659–4664.
33 C. Y. Liu, P. Jia and L. Wu, *Sens. Actuators, B*, 2019, **297**, 126731.
34 L. F. Pang, Y. M. Zhou and W. L. Gao, *RSC Adv.*, 2016, **6**, 105795–105800.
35 L. Shi, H. J. Yu and X. Q. Zeng, *New J. Chem.*, 2020, **44**, 6232–6237.
36 X. Wang, Y. M. Zhou and C. G. Xu, *Spectrochim. Acta, Part A*, 2018, **203**, 415–420.
37 L. L. Wu, Q. Y. Yang and L. Y. Liu, *Chem. Commun.*, 2018, **54**(61), 8522–8525.
38 D. Q. Lu, L. Y. Zhou, R. W. Wang, X. B. Zhang, L. He, J. Zhang, X. X. Hu and W. H. Tan, *Sens. Actuators, B*, 2017, **250**, 259.
39 X. Y. Li, L. Wu, Z. Y. Zhao, C. Y. Liu and B. C. Zhu, *RSC Adv.*, 2019, **9**, 4659.
40 B. C. Zhu, L. Wu, M. Zhang, Z. Y. Zhao, Z. K. Wang, Q. X. Duan, P. Jia, L. Li, H. C. Zhu and C. Y. Liu, *Sens. Actuators, B*, 2018, **267**, 589.
41 B. C. Zhu, P. Li, W. Shu, X. Wang, C. Y. Liu, Y. Wang, Z. K. Wang, Y. W. Wang and B. Tang, *Anal. Chem.*, 2016, **88**, 12532.
42 G. J. Mao, T. T. Wei, X. X. Wang, S. S. Huan, D. Q. Lu, J. Zhang, X. B. Zhang, W. H. Tan, G. L. Shen and R. Q. Yu, *Anal. Chem.*, 2013, **85**, 7875.
43 *Standardization Administration of the People's Republic of China (SAC) has set the drinking water sanitary standard (GB5749-2006)*, http://www.sac.gov.cn/.
44 *Standardization Administration of the People's Republic of China (SAC) has set Discharge standards of water pollutants of medical organization (GB18466-2016)*, http://www.sac.gov.cn/.